Influence of etching modes on the morphology and composition of the surface of multilayer porous silicon

© *A.S. Lenshin* [1,2], *Ya.A. Peshkov* [1], *O.V. Chernousova* [2], *K.A. Barkov* [1], *S.V. Kannykin* [1]

[1] Voronezh State University,
394018 Voronezh, Russia
[2] Voronezh State University of Engineering Technologies,
394000 Voronezh, Russia

E-mail: lenshinas@mail.ru

Based on X-ray reflectometry and ultrasoft X-ray spectroscopy data, the opportunity of controlling surface porosity using multi-stage electrochemical etching modes is presented. It is presented how, with an increase in the porosity index of the near-surface layer, the morphology changes and the degree of oxidation of multilayer porous silicon samples increases.

Keywords: porous silicon, X-ray reflectometry, porosity.

1. Introduction

Porous silicon (*por*-Si) is a complex multiphase material, the composition and functional properties of which strongly depend on its porosity [1–3]. It is known that, depending on the preparation method, *por*-Si can have an extremely large specific pore surface area, high reactivity and intense photoluminescence in the visual wavelength range. The opportunities of creating gas sensors, optical sensors, and humidity sensors have been demonstrated using porous silicon structures. The use of multi-stage modes of formation of a porous layer on single crystal silicon can also be promising for fine-tuning its surface and volumetric functional characteristics for the purpose of further formation on its surface of thin layers of such modern nanoelectronic materials as metal oxide structures or structures of type $A^{III}B^{V}$ [4,5].

X-ray reflectometry (XRR) occupies a special place in the methods for calculating the porosity of *por*-Si. The advantage of using XRR is that it allows to measure the porosity of the near-surface layer of the sample, which determines many of the functional properties of *por*-Si. In addition, in works [7,8] it was revealed that the porosity index also depends on the depth of analysis and on sample exposure to the atmosphere. The purpose of this work is to develop a technique for forming samples of multilayer porous silicon with different porosities and to analyze the relationship between the porosity index of near-surface layers and their composition.

2. Experiment procedure

Porous silicon samples were obtained by electrochemical etching (ECE) of single crystal silicon wafers doped with phosphorus in a solution of fluoric acid and isopropyl alcohol [9]. The porosity of the samples was varied by a stepwise change in the current density during the ECE process; the etching solution did not change (see the Table). The studies were carried out 6 months after obtaining the samples. To measure porosity values, X-ray reflectometry of *por*-Si samples was carried out using an ARL X'TRA X-ray diffractometer in Bragg-Brentano geometry (CuK_α). The position of the critical angle of total external reflection (TER) is proportional to the average electron density of the medium [10]. Therefore, knowledge of the critical TER angle of porous silicon $\theta_{c\text{-PS}}$ and silicon substrate $\theta_{c\text{-Si}}$ allows to calculate the porosity index using the relationship: $P(\%) = \left[1 - (\theta_{c\text{-PS}}/\theta_{c\text{-Si}})^2\right] \cdot 100$ [11]. The penetration depth of X-ray radiation into *por*-Si near the critical angle is several tens of nanometers [8,12]. Analysis of sample chips was carried out by scanning electron microscopy (SEM) on a JEOL–JSM 6380LV device.

Ultrasoft X-ray emission spectroscopy USXES is used to study the electronic structure of disordered systems [13]. Si $L_{2,3}$-spectra of porous silicon samples were obtained on a RSM-500 X-ray spectrometer-monochromator. The depth of sample analysis was 60 nm, which is comparable to the depth of analysis using the XRR method. At simulation of the Si $L_{2,3}$ spectra of the *por*-Si samples, the reference spectra *c*-Si, *a*-Si:H, low-ordinated silicon Si_{lc}, SiO_x ($x \sim 1.3$) and SiO_2 [12,13] were used. The simulation error did not exceed KD 10%.

3. Results and discussion

Figure 1 presents SEM images of sample chips of single- and multilayer porous silicon with different surface porosities. On sample chips, we can observe that an
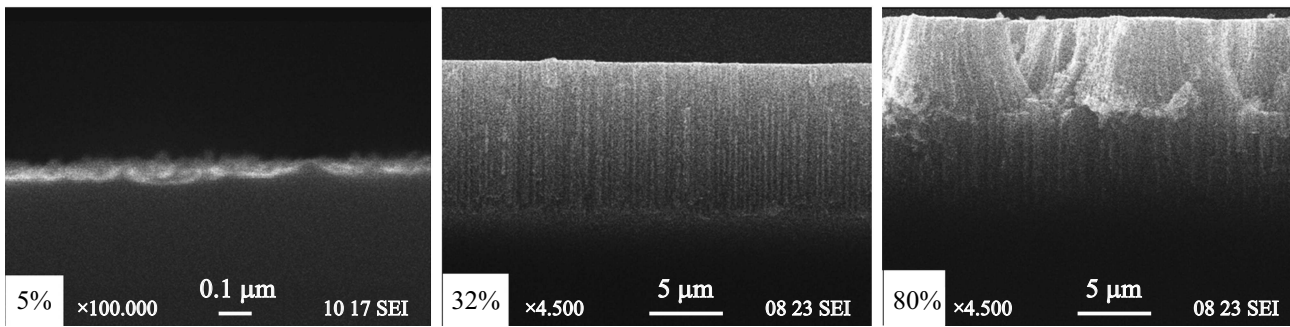
Figure 1. SEM images of *por*-Si sample chips with different porosities.
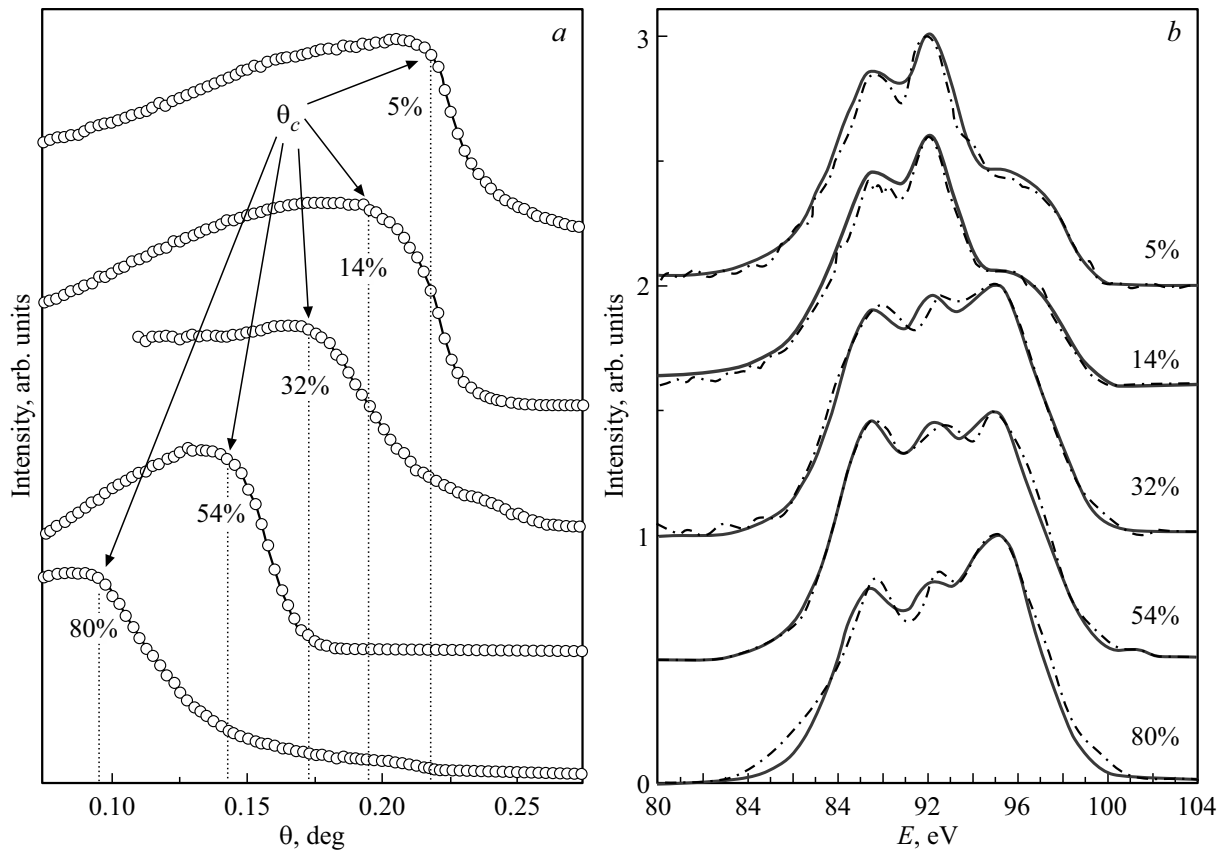

Figure 2. XRR profiles of *por*-Si samples and silicon substrate (*a*). The dotted lines indicate the critical angles of total external reflection and porosity values. USXES — spectra of porous silicon samples of various porosities (*b*).

increase in the ECE current density leads to an increase in the thickness of the porous layer and pore diameter, while a stepwise change in the current density during the ECE process leads to the formation of a multilayer porous structure and allows to control the surface porosity within a wide range (see the Table).

Figure 2, *a* shows XRR curves and calculated porosity indicators of the surface layer of *por*-Si samples obtained in different modes. The experimental measurement of the critical angle for a single crystal silicon substrate was $0.223°$, which is in good agreement with previously obtained results and with theoretical calculations ($\theta_{c\text{-Si}} \approx 0.22°$ for

$\lambda = 1.54\,\text{Å}$) [11]. The results of calculating the porosity index *por*-Si demonstrate that controlling the ECE current density allows to obtain samples with porosity in the range from 5 to 80%.

Figure 2, *b* shows USXES Si $L_{2,3}$ spectra of porous silicon, taken at a sample analysis depth of 60 nm. The results of simulation of the phase composition of *por*-Si samples using the spectra of reference compounds are presented in the Table.

The results of studying the composition of porous silicon with different porosity factors using the USXES method showed that after long-term storage in the atmosphere,

Distribution of phase composition components in percentage terms for porous silicon samples

Density of the current j, mA/cm^2	Time etching, min	P, %	c-Si, %	a-Si:H/Si$_{lc}$, %	SiO$_x$, %	SiO$_2$, %	Error, %
25	9	5	100	0	0	0	5
50	9	32	34	15	3	48	7
50/20/20	9	54	36	7	25	32	4
20/50/20	9	80	29	8	0	62	8

por-Si contains phases of crystalline, amorphous and disordered silicon, as well as silicon suboxide and dioxide. Samples with a low porosity index are close in composition to crystalline silicon, their spectra coincide by more than 95% with the spectrum of the reference c-Si, and for samples with porosity $> 30\%$ the proportion of oxide phases in the composition increases with the porosity index. The percentage ratio of unoxidized to oxidized phases in the samples decreased from $\sim 50/50$ to $35/65$ with an increase in surface porosity from 30 to 80% (see the Table). This is explained by the larger pore surface area exposed to oxidation during exposure to atmosphere.

4. Conclusion

Thus, the work shows that it is possible to control the porosity of the *por*-surface within a wide range, and how, with an increase in the porosity index of the near-surface layer, the morphology changes and the degree of oxidation of multilayer porous silicon samples increases. The data correlate well with the qualitative results that we obtained for porous silicon at the initial stages of natural aging, as well as for micro-, meso- and nanoporous silicon in the works [12,13].

Conflict of interest

The authors declare that they have no conflict of interest.

References

[1] L. Canham. Handbook of Porous Silicon (Springer, C.H., 2014) p. 733. DOI: 10.1007/978-3-319-05744-6
[2] C. Pacholski. Sensors, **13**, 4694 (2013). DOI: 10.3390/s130404694
[3] R. Moretta, L. De Stefano, M. Terracciano, I. Rea. Sensors, **21**, 1336 (2021). DOI: 10.3390/s21041336
[4] L.T. Canham. Appl. Phys. Lett., **57**, 1046 (1990). DOI: 10.1063/1.103561
[5] P.V. Seredin, A.S. Lenshin, A.M. Mizerov, H. Leiste, M. Rinke. Appl. Surf. Sci., **476**, 1049 (2019). https://doi.org/10.1016/j.apsusc.2019.01.239
[6] S. Asgharizadeh, M. Sutton, K. Robbie, T. Brown. Phys. Rev. B, **79**, 125405 (2009). DOI: 10.1103/PhysRevB.79.125405
[7] M. Servidori, C. Ferrero, S. Lequien, S. Milita, A. Parisini, R. Romestain, S. Sama, S. Setzu, D. Thiaudiere. Solid State Commun., **118**, 85 (2001). DOI: 10.1016/S0038-1098(01)00036-9
[8] L.A. Balagurov, V.F. Pavlov, E.A. Petrova, G.P. Boronina. Semiconductors, **31**, 815 (1997). DOI: 10.1134/1.1187259
[9] A.S. Lenshin, A.N. Lukin, Ya.A. Peshkov, S.V. Kannykin, B.L. Agapov, P.V. Seredin, E.P. Domashevskaya. Condens. Matter Interphases, **23**, 41 (2021). DOI: 10.17308/kcmf.2021.23/3300
[10] A.S. Lenshin, Ya.A. Peshkov, M.V. Grechkina, S.V. Kannykin, Yu.A. Yurakov. J. Phys.: Conf. Ser., **1984**, 012018 (2021). DOI: 10.1088/1742-6596/1984/1/012018
[11] D. Buttard, G. Dolino, D. Bellet, T. Baumbach, F. Rieutord. Solid State Commun., **109**, 1 (1998). DOI: 10.1016/S0038-1098(98)00531-6
[12] A. Lenshin, Ya. Peshkov, K. Velichko, S. Kannykin. Int. Conf. on Information Technology and Nanotechnology (ITNT) (20−24 September 2021, Samara, Russian Federation, 1 (2021). DOI: 10.1109/ITNT52450.2021.9649173
[13] A.S. Lenshin, V.M. Kashkarov, E.P. Domashevskaya, A.N. Bel'tyukov, F.Z. Gil'mutdinov. Appl. Surf. Sci., **359**, 550 (2015).

Translated by Ego Translating